Current Biology 16, 2143–2149, November 7, 2006 ©2006 Elsevier Ltd All rights reserved DOI 10.1016/j.cub.2006.08.091

Report

Vectorial Information for *Arabidopsis* Planar Polarity Is Mediated by Combined *AUX1*, *EIN2*, and *GNOM* Activity

Urs Fischer,[1] Yoshihisa Ikeda,[1] Karin Ljung,[1] Olivier Serralbo,[2,4] Manoj Singh,[3] Renze Heidstra,[2] Klaus Palme,[3] Ben Scheres,[2] and Markus Grebe[1,*]

[1] Umeå Plant Science Centre
Department of Forest Genetics and Plant Physiology
Swedish University of Agricultural Sciences
90183 Umeå
Sweden

[2] Department of Molecular Genetics
Utrecht University
Padualaan 8
3584 CH Utrecht
The Netherlands

[3] Institute of Biology II
University of Freiburg
Schänzlestrasse 1
79104 Freiburg
Germany

Summary

Cell polarity is commonly coordinated within the plane of a single tissue layer (planar polarity), and hair positioning has been exploited as a simple marker for planar polarization of animal epithelia [1]. The root epidermis of the plant *Arabidopsis* similarly reveals planar polarity of hair localization close to root tip-oriented (basal) ends of hair-forming cells [2–4]. Hair position is directed toward a concentration maximum of the hormone auxin in the root tip [4, 5], but mechanisms driving this plant-specific planar polarity remain elusive. Here, we report that combinatorial action of the auxin influx carrier *AUX1* [6, 7], *ETHYLENE-INSENSITIVE2* (*EIN2*) [8], and *GNOM* [9] genes mediates the vector for coordinate hair positioning. In *aux1*;*ein2*;*gnom*^{eb} triple mutant roots, hairs display axial (apical or basal) instead of coordinate polar (basal) position, and recruitment of Rho-of-Plant (ROP) GTPases to the hair initiation site [10, 11] reveals the same polar-to-axial switch. The auxin concentration gradient is virtually abolished in *aux1*;*ein2*;*gnom*^{eb} roots, where locally applied auxin can coordinate hair positioning. Moreover, auxin overproduction in sectors of wild-type roots enhances planar ROP and hair polarity over long and short distances. Hence, auxin may provide vectorial information for planar polarity that requires combinatorial *AUX1*, *EIN2*, and *GNOM* activity upstream of ROP positioning.

*Correspondence: markus.grebe@genfys.slu.se
[4] Present address: Developmental Biology Institute of Marseille (IBDM), Université de la Méditerranée, Campus de Luminy Case 907, 13288 Marseille, Cedex 09, France.

Results and Discussion

Directional information for orientation of cells within the tissue layer is critical at multiple stages of plant and animal development [1–5, 9–13]. In animals, coordinate polar alignment of single cells or multicellular units in the plane of the epithelial layer is referred to as planar polarity [1]. Advantages of a simple single-cell layer system providing a direct morphological read-out for planar polarity have not been systematically exploited in plants. The *Arabidopsis* root epidermis represents such a system, where, similar to coordinate polar arrangement of *Drosophila* wing hairs [1], root hairs emerge close to root tip-oriented (basal) ends of hair-forming cells (trichoblasts) [2–4]. Root hair positioning displays planar polarity in its strictest sense, a common polar orientation of cells in the plane of a single tissue layer [2]. This does not necessarily imply that the same mechanisms regulate planar polarity in plants and animals. Indeed, application of the plant hormones auxin or ethylene hyperpolarizes root hair initiation to a basal-most position [3, 4] (Figures S1A and S1B in the Supplemental Data available online), and apical shifts of hair position are observed upon pharmacological interference with auxin transport [3–5]. The auxin influx carrier AUX1 contributes to hair positioning, and the process is highly sensitive to the vesicle transport inhibitor brefeldin A (BFA) [4]. Weak hair position defects in *aux1* mutants suggest that additional factors must be involved [4], and a requirement of direct BFA target proteins for planar polarity remains to be demonstrated by loss-of-function studies.

Here, we first addressed whether GNOM, a direct BFA target in *Arabidopsis* [9, 13], contributes to polar root hair positioning. *gnom* loss of function causes a rootless phenotype, prompting us to observe consequences of partially reduced *GNOM* activity in a viable *gnom* transheterozygous mutant (*gnom*$^{emb30\text{-}1}$/*gnom*^{B4049}; *gnom*^{eb}) [14] and the weak *gnom*^{van7} allele [15]. Both *gnom* mutants display an apical shift of root hair position along the trichoblast (Figures 1A–1D, 1F, and 1G), revealing the requirement of *GNOM* for coordinate root hair positioning. To obtain insight into auxin and ethylene action in relation to *GNOM* function, we grew *gnom*^{eb} seedlings on media containing the auxin influx carrier substrate 2,4-dichlorophenoxyacetic acid (2,4-D) [16] or the ethylene precursor 1-amino-cyclopropane-1-carboxylate (ACC). Both treatments induce hair shifts to a more basal position in *gnom*^{eb} (Figures 1E, 1H, and 1I), suggesting that auxin influx and ethylene modulation of planar polarity remain partially active in *gnom*^{eb}.

To establish whether reduced ethylene responsiveness affects hair position, we examined *ethylene insensitive2* (*ein2*) mutants thought to confer complete ethylene insensitivity [8]. Strong *ein2* loss-of-function alleles, including the null allele *ein2-T* (Figure S2A, see Supplemental Experimental Procedures), display significant apical shifts of hair initiation (Figures 1J and 1O; Figures

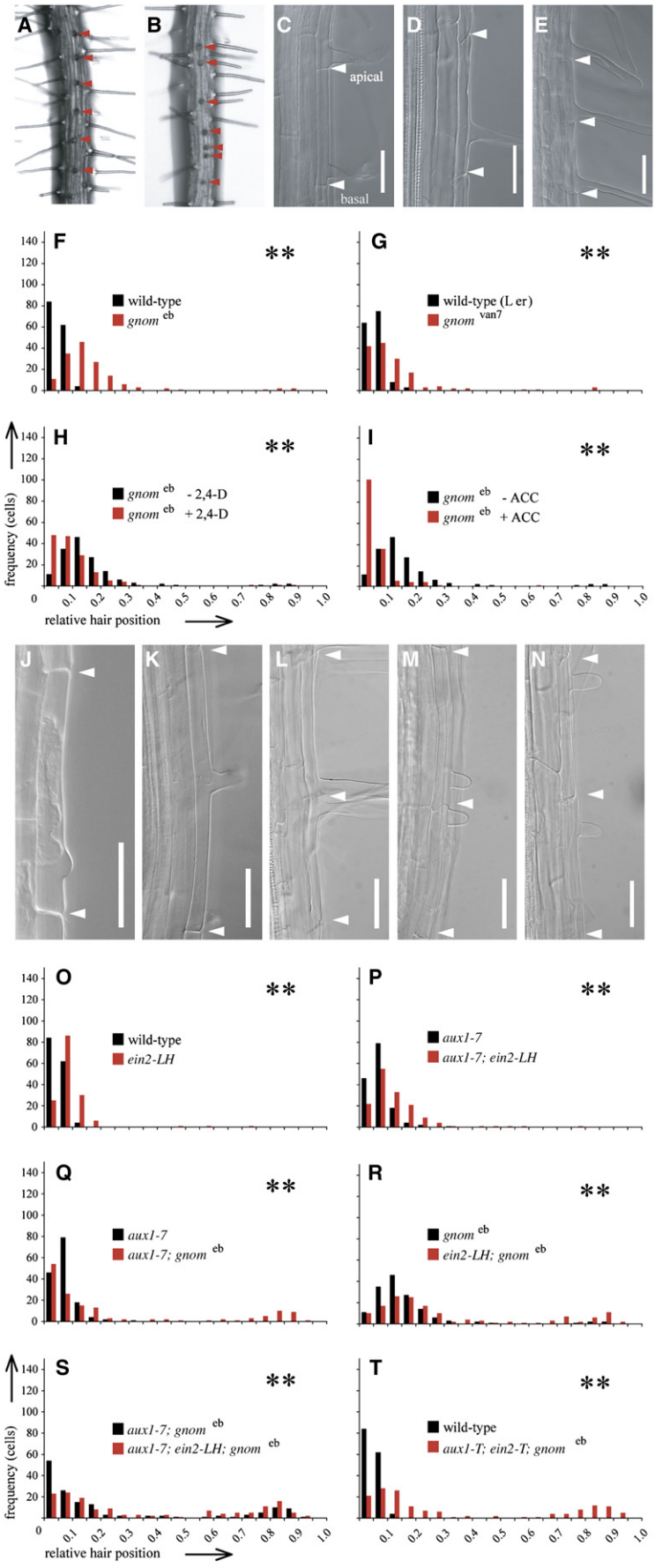

Figure 1. Combinatorial *AUX1, EIN2*, and *GNOM* Activity Mediates the Vector for Planar Root Hair Orientation

(A and B) Root hair position in wild-type Columbia (Col) (A) and *gnom*^{eb} (B) transheterozygote roots. Red arrowheads, root hairs.

(C–E) Root hair position in Col hair cells (C), *gnom*^{eb} (D), 20 nM 2,4-D *gnom*^{eb} (E). White arrowheads, cell walls. Scale bars represent 50 μm.

(F–I and O–T) Frequency distributions of relative hair position determined on 150 root hair cells from 30 roots per genotype or treatment. Relative hair position is given between 0 = basal and 1 = apical cell wall (cf. [C]). Genotypes and treatments are indicated. Note: (H) 20 nM 2,4-D (2,4-D), (I) 5 μM ACC (ACC). Significance level for independence of distributions is $p < 0.05$. p values are indicated as highly significant $^{**}p < 0.001$ on a basis of n = 150 cells. For exact p values, see Table S3.

(J–N) Root hair position in *ein2-T* (J), *aux1-22;ein2-T* (K), *aux1-7;gnom*^{eb} (L), *ein2-LH*; *gnom*^{eb} (M), *aux1-7;ein2-LH;gnom*^{eb} (N). *ein2-LH* isolated by Hobbie et al. [17]. White arrowheads, cell walls. Scale bars represent 50 μm.

S1C and S1D) and double hair formation at higher frequency than wild-type (Table S1, Figure S1E), suggesting that *EIN2* contributes to hair positioning. To observe consequences of combined *AUX1* and *EIN2* loss of function, we analyzed *aux1;ein2* double mutants including the *aux1-T;ein2-T* null alleles (Figures S2A and S2B). *aux1;ein2* double mutants display enhanced apical shifting of hair initiation (Figures 1K and 1P; Figures S1F and S1G) and a three times higher number of double hairs than respective single mutants (Table S1), suggesting synergistic action of *AUX1* and *EIN2* on planar epidermal polarity.

We next aimed to establish the functional relationship between *AUX1*, *EIN2*, and *GNOM* and generated respective double and triple mutants with *gnom*^{eb}. *aux1;gnom*^{eb} and *ein2;gnom*^{eb} double mutants reveal a higher proportion of hairs emerging from apical ends of cells (Figures 1L, 1M, 1Q, and 1R) compared to the single mutants or transheterozygotes (Figures 1J, 1K, 1O, 1Q, and 1R). These results suggest that *GNOM* is active in the absence of *AUX1* or *EIN2* and that planar polarity requires the combined activity of the three genes. Consistently, distribution of GNOM-GFP remains undisturbed in *aux1, ein2* single and *aux1;ein2* double mutants (Figures S3A–S3D). Likewise, *gnom*^{eb} or *ein2* mutations do not perturb subcellular localization of hemagglutinin (HA)-tagged AUX1 protein (Figures S3E–S3J). Although BFA treatment affects HA-AUX1 localization in root cells [4], HA-AUX1 distribution appears mostly independent of GNOM-mediated BFA effects (Figures S4A–S4F).

Intriguingly, the hairs of *aux1;ein2;gnom*^{eb} triple mutants preferentially emerge from apical or basal trichoblast ends (Figures 1N, 1S, and 1T), suggesting that trichoblasts do not correctly bias hair positioning toward the polarity cue or that the cue itself is perturbed in the triple mutant. Several lines of evidence support that this cue displays the vectorial characteristic direction and magnitude. First, consecutive removal of *AUX1* and *EIN2* and reduction of *GNOM* activity gradually reduces the bias to orient hairs to basal ends of cells (Figures 1O–1S). Second, hair position can be gradually hyperpolarized by external auxin [3, 4] or depolarized by exogenous BFA application, in a concentration-dependent manner [4]. Together, our findings strongly suggest that combinatorial activity of the *AUX1*, *EIN2*, and *GNOM* genes mediates the vectorial cue for planar root hair positioning.

To elucidate at which level *AUX1*, *EIN2*, and *GNOM* action converges, we employed localization of Rho-of-plant (ROP) small GTPases as an early polarity marker for the hair initiation site [10, 11] (Figure 2; Figure S5). ROP2 may regulate hair initiation, because its overexpression causes formation of multiple hairs from trichoblasts [11]. We observe clear apical shifts of ROP localization in *gnom*^{eb} (Figure 2B) when compared to wild-type (Figure 2A), demonstrating that *GNOM* is required for planar ROP polarity. Furthermore, analyses of *aux1*, *ein2* single, *aux1;ein2* double, and *aux1;ein2;gnom*^{eb} triple mutants reveal apical shifts of ROP position (Figures 2C–2F). Defects are most pronounced in *aux1;ein2;gnom*^{eb} triple mutants, where ROP preferentially localizes to either apical or basal trichoblast ends (Figure 2F; Figure S5E), suggesting that combined action of *AUX1*, *EIN2*, and *GNOM* on planar polarity converges prior to coordinate ROP positioning.

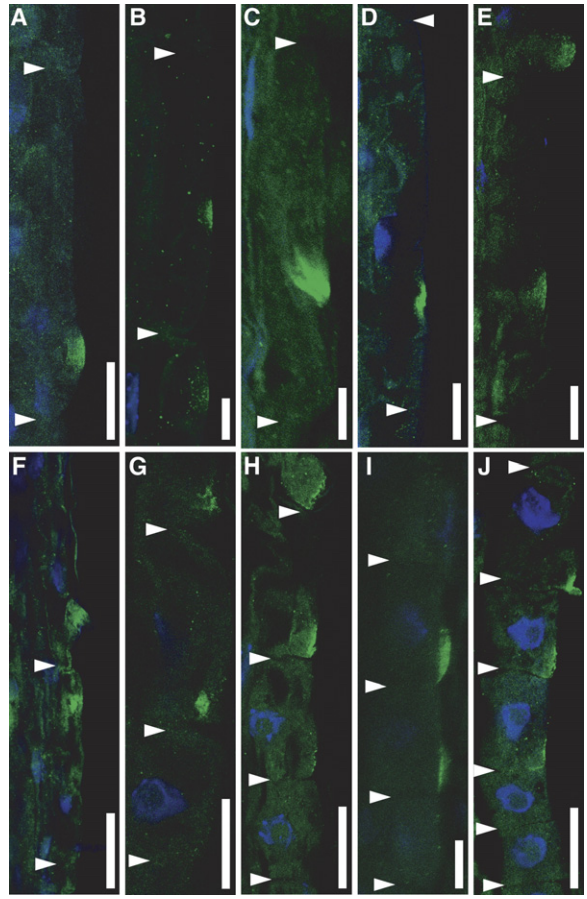

Figure 2. Combinatorial Action of *AUX1*, *EIN2*, and *GNOM* Converges Prior to Coordinate Rho-of-plant Positioning

ROP immunolocalization (green) in wild-type and mutant trichoblasts employing anti-ROP serum [10]. DAPI-stained nuclei (blue). ROP localization in wild-type (Col) (A), *gnom*^{eb} (B), *aux1-T* (C), *ein2-LH* (D), *aux1-7;ein2-LH* (E), *aux1-7;ein2-LH;gnom*^{eb} (F), 20 nM 2,4-D Col (G), 5 μM ACC Col (H), *sur2-1* (I), and *eto3* (J). Cell walls, white arrowheads. Scale bars represent 20 μm. n = 20–35 roots per genotype or treatment. For quantitative data on ROP position and cell length, see Figure S5 and Table S2.

Our results indicate that polar bias may be enhanced by auxin and ethylene. To address effects of increased levels of these hormones on ROP position, we grew plants on agar containing 20 nM 2,4-D or 5 μM ACC. Under these conditions, the auxin-response maximum revealed by the reporter *DR5rev::GFP* [18] is locally increased in the root tip but not in elongating epidermal cells (Figure S6), suggesting that exogenous hormone application at these concentrations enhances the auxin-response gradient. In contrast to the untreated wild-type (Figure 2A), ROP localization occurs at basalmost ends of trichoblasts and early during longitudinal cell expansion in roots grown on medium containing 20 nM 2,4-D (Figure 2G) or 5 μM ACC (Figure 2H) (see also Figure S5 and Table S2). Similarly, auxin-overproducing *superroot2-1* (*sur2-1*) and *ethylene overproducer3* (*eto3*) mutants [19, 20] display basally shifted ROP localization (Figures 2I and 2J, Figure S5), demonstrating that

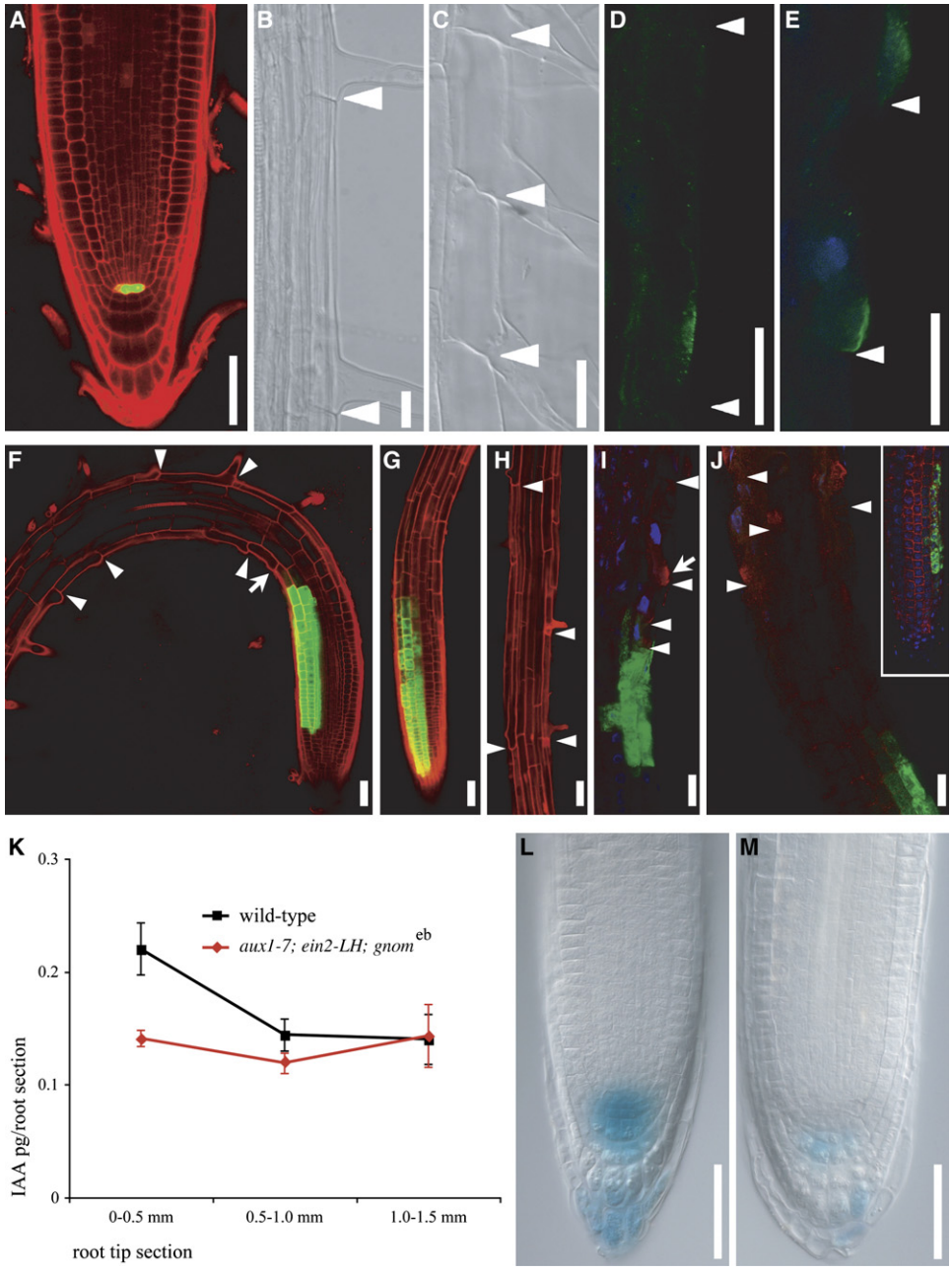

Figure 3. Sector Analyses of Long- and Short-Range Auxin Action on ROP and Root Hair Position

(A) *pWOX5::ER-GFP* expression in quiescent center cells [22].

(B and C) Root hair position in *pWOX5::iaaH* line on IAM-free medium (B), 100 nM IAM (C). For quantitative analyses of 150 cells, see Figures S7G and S7H. White arrowheads, cell walls.

(D and E) Anti-ROP (green) immunolocalization in trichoblasts from *pWOX5::iaaH* line on IAM-free medium (D), 100 nM IAM (E). White arrowheads, cell walls.

(D, E, I, and J) DAPI-stained nuclei (blue).

(F–J) Sector analyses of short-range auxin effects on hair position next to ER-GFP-marked *iaaH* expression sectors (green). White arrowheads, cell walls.

(F–H) Propidium iodide-stained cell walls (red). (F) Epidermal *iaaH* sector 24 hr after heat shock in a root on 100 nM IAM. Hair bulge initiating from a basal-most position during early cell elongation, at a distance of one cell to the border of the sector (arrow). Note, hairs initiate from basal-most positions in proximity to the sector and roots bend to the flank of *iaah* induction, not observed in (G, H) root with sector on IAM-free medium. (H) Early differentiation zone of the root in (G). Note, normal polarity of hair position. For quantitative analyses of clones in meristematic, meristematic/elongating, elongating, root hair initiating, and differentiated epidermal cells, see Figure S7.

(I) ROP immunolocalization (red) in vicinity of an epidermal *iaaH* sector (green) in a root on 100 nM IAM. Hyperpolar ROP accumulation occurs in a cell close to the border of the sector (arrow).

(J) ROP localization (red) at the hair initiation site is only observed at a distance from the epidermal *iaaH* sector (green) on IAM-free medium. Full sector (green) in relation to the root tip with meristematic ROP label (red).

(K–M) Auxin concentration gradient and auxin responses in root tips.

externally applied or endogenously overproduced auxin and ethylene hyperpolarize ROP position.

Auxin overproduction may affect planar polarity more directly than enhanced ethylene biosynthesis, since ethylene signaling can act upstream of auxin biosynthesis in *Arabidopsis* roots [21]. A polarizing factor that may act via a gradient should exert its effects over long distances from its concentration maximum as well as in target cells [1]. We investigated long-range effects of local auxin overproduction in plants expressing the bacterial auxin biosynthesis gene *iaaH* in quiescent center cells under control of the *pWOX5* promoter (Figure 3A, *pWOX5::ER-GFP*) [22], at a distance of about one millimeter from the first emerging root hairs [23]. iaaH catalyzes conversion of inactive indole-3-acetamide (IAM) to the biologically active auxin indole-3-acetic acid (IAA). *pWOX5::iaaH* expression hyperpolarizes hair and ROP position in plants grown on IAM (Figures 3C and 3E), compared to *pWOX5::iaaH* plants grown on IAM-free medium (Figures 3B and 3D; Figure S7G) or wild-type grown on IAM (Figure S7H; and data not shown). Thus, auxin overproduced in proximity to its endogenous concentration maximum confers long-range hyperpolarizing activity on planar polarity.

To address short-range effects of local auxin overproduction, we expressed *iaaH* in positively ER-GFP-marked sectors. This was achieved by modifying a heat shock-inducible, CRE/lox recombination-based clonal activation system [24] for *iaaH* expression. We first analyzed hair position in proximity to epidermal *iaaH* sectors spanning meristematic and the first elongating trichoblasts. In the vicinity of sectors from plants grown on IAM-containing medium, root hair formation occurs from a basal-most position of trichoblasts, starting in cells within the elongation zone (Figure 3F, arrow; Figures S7B and S7J). Similar results are obtained for hair positioning in trichoblast cell files harboring *iaaH* expression sectors in meristematic or elongating epidermal cells (Figures S7A, S7C, S7I, and S7K), but not when sectors are induced above the zone of root hair initiation or in differentiated hair cells (Figures S7D–S7F, S7L, and S7M), suggesting that auxin can act on planar polarity from meristematic and directly in elongating epidermal cells. Such effects are observed neither in roots with sectors induced on IAM-free medium (Figures 3G and 3H; Figure S7O) nor in noninduced roots on IAM-containing medium (Figure S7J). Strikingly, in roots grown on IAM, hyperpolar ROP accumulation is observed in elongation zone cells at a distance as close as one cell to the apical border of the sector (Figure 3I, arrow), but not close to sectors in roots on IAM-free medium (Figure 3J, inset), showing that auxin can induce polar ROP recruitment over short distances. Together, our results demonstrate long- and short-range as well as direct auxin action on planar epidermal polarity in elongating cells.

We next addressed whether *aux1;ein2;gnom*^{eb} mutants display an altered endogenous auxin concentration gradient. Analysis of free IAA over the first three 500 μm sections of the root tip reveals significant reduction of IAA concentration in the first millimeter of *aux1;ein2;gnom*^{eb} roots, compared to wild-type (Figure 3K). Consistently, in comparison to wild-type expressing the auxin-responsive *DR5::GUS* reporter (Figure 3L), *aux1;ein2;gnom*^{eb} root tips display a decreased auxin response (Figure 3M). Intriguingly, the slope of the auxin concentration gradient is almost lost in *aux1;ein2;gnom*^{eb} (Figure 3K), correlating defects in planar hair position with a strongly diminished auxin gradient.

These observations prompted us to examine whether re-establishment of an auxin concentration maximum could be instructive in coordinating planar polarity. To test this, we infiltrated Sephadex beads with the membrane-permeable auxin 1-naphthalene-acetic acid (1-NAA, 1 mM solution) and locally applied them to the tip or early elongation zone of *aux1;ein2;gnom*^{eb}*;DR5::GUS* roots. A local auxin-response maximum can be induced around the site of bead application (Figures 4A, 4B, and 4I), which is not observed when the inactive structural analog 2-NAA is applied (Figures 4C and 4D). After 18 hr of 1-NAA application, root hairs have emerged from trichoblasts located above beads placed on the root tip (Figures 4E and 4G) as well as from below and above beads placed on the early elongation zone (Figures 4F, 4H, 4I, and 4J). In both cases, hair position is coordinately biased toward the local auxin source (Figure 4I, 4J, and 4K) that has generated an auxin-response gradient (Figure 4I), while locally applied 2-NAA does not coordinate root hair position (Figure 4L). These results suggest that a local auxin source is sufficient to introduce directional bias to single-cell polarity within the plane of the epidermal layer.

The strongly reduced coordination of polar hair positioning and the impaired auxin gradient in *aux1;ein2;gnom*^{eb} roots, long- and short-range auxin action on planar polarity in elongating cells, and the ability of a local auxin source to partially coordinate single-cell polarity in *aux1;ein2;gnom*^{eb} triple mutants suggest that auxin provides one cue contributing to the planar polarity vector.

Coordinate polar epidermal localization of the PIN1 auxin efflux carrier in inflorescences is regulated by the PINOID protein kinase [12]. Unlike the proposed binary switch character of PINOID action on PIN1 orientation [12], the choice between apical and basal hair position reflects a gradual decision between axial alignment and coordinate polar hair orientation (Figures 1O–1T). The apical localization of epidermally expressed PIN proteins detected by anti-PIN1 and anti-PIN2 sera [22] is not altered in *aux1;ein2;gnom*^{eb} root epidermal cells (Figures S8A–S8E), suggesting that establishment of planar polarity involves mechanisms distinct from apical epidermal PIN polarity. We do not observe planar hair polarity defects in *pin1*, *pin2* single, *pin1;pin2* double, or *pin2;pin4;pin7* triple mutants and only minute, weakly significant changes in *pin1;pin2;pin3;pin7* quadruple

(K) Detection of free IAA in three 0.5 mm sections of wild-type and *aux1-7;ein2-LH;gnom*^{eb} root tips. Bars indicate ± SD from averages of three independent experiments. Significance level for differences between samples is $p < 0.05$. p values are $p = 0.003$ for 0–0.5 mm, $p = 0.033$ for 0.5–1.0 mm, and $p = 0.451$ for 1.0–1.5 mm sections.

(L and M) *DR5::GUS* expression in root tips of wild-type (L) and *aux1-7;ein2-LH;gnom*^{eb} (M) roots. n = 30 roots, each.

Scale bars represent 50 μm in (A), (F)–(H), (L), and (M) and 20 μm in (B)–(E), (I), and (J).

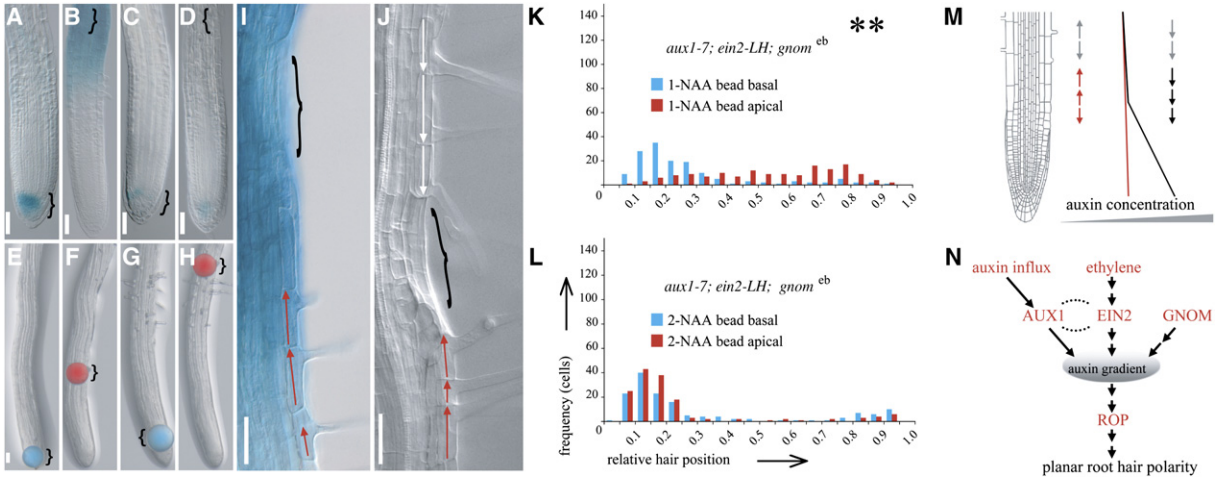

Figure 4. Auxin Can Confer Directional Bias to Planar Polarity

(A to J) Parentheses indicate bead positions. Scale bars represent 50 μm.

(A–D, I) *DR5::GUS* expression in *aux1-7*;*ein2-LH*;*gnom*^{eb};*DR5::GUS* roots treated for 18 hr with 1 mM 1-NAA (A, B, and I) or 1 mM 2-NAA infiltrated Sephadex-G50 beads (C and D).

(E–H) 1 mM 1-NAA beads at the start (E and F) and the end (G and H) of the treatment.

(E and G) Bead (false blue) applied to the root tip at t = 0 (E) and observed after 18 hr (G).

(F and H) Bead (false red) applied to the early elongation zone at t = 0 (F) and observed after 18 hr (H).

(I) Auxin-response gradient (blue) around the site of bead application (parenthesis) and directionality of root hair position (red arrows).

(J) Root hair position (red and white arrows) oriented toward the site of bead application (parenthesis) on early elongation zone cells after 18 hr of 1-NAA.

(K and L) Frequency distributions of relative hair position in *aux1-7*;*ein2-LH*;*gnom*^{eb} after 18 hr 1-NAA bead on the root tip (basal) or the early elongation zone (apical) (K), 2-NAA bead on the root tip (basal) or the early elongation zone (apical) (L). Hair position has been determined on cells directly above beads applied to the root tip (blue) or directly below beads applied to the early elongation zone (red). n = 150 hair cells derived from 30 1-NAA-treated roots (K) or 50 2-NAA-treated roots (J). Significance levels as in Figure 1.

(M) Hypothetic model for planar root hair positioning. Trichoblasts polarize hair initiation (black arrows) toward maximum concentration of the auxin gradient. Gradient flattening correlates with loss of coordinated polarity (red arrows). Gray arrows mark orientation of differentiated hair cells.

(N) Genetic relationships during establishment of planar polarity and presumptive relation to the auxin gradient. Dotted lines indicate synergistic action.

mutants (Figures S8I–S8L; [4]), indicating that planar polarity does not largely rely on activity of these PIN auxin efflux carrier components.

During planar wing hair placement in *Drosophila*, the *frizzled* pathway transmits short-range signals to Rho/Rac GTPases that regulate actin organization during prehair formation [1, 25]. The *Arabidopsis* genome lacks core components of the *frizzled* pathway (M.G., data not shown), but root hair positioning also involves ROP and actin as downstream components [10, 11]. Our findings demonstrate that auxin can modulate ROP and hair positioning over long distances, short distances, and in elongating cells and that *AUX1*, *EIN2*, and *GNOM* mediate auxin-related vectorial information for coordinate ROP localization. They further suggest that a mobile auxin signal contributes to the planar polarity vector. This likely involves AUX1-dependent basipetal auxin influx from the concentration maximum to elongating epidermal cells [26]. Our present study provides an initial mechanistic framework of components that confer vectorial information to planar root hair positioning (Figures 4M and 4N). The modulation of the planar polarity vector by the endocytic GNOM protein suggests an involvement of endocytosis that can be inhibited by auxin in root epidermal cells [27]. Future detailed studies may address how specifically auxin influx, ethylene signaling, and endocytosis interact to generate vectorial information in the plane of the tissue layer. Such studies may also reveal whether intra- or intercellular auxin gradients are instructive in establishment of planar polarity and whether the process requires additional efflux components or relay mechanisms. Ongoing screens for mutations affecting root hair positioning in our laboratory should help to identify new factors and mechanisms regulating planar polarity in plants.

Supplemental Data

Supplemental Data include eight figures, three tables, and Supplemental Experimental Procedures and can be found with this article online at http://www.current-biology.com/cgi/content/full/16/21/2143/DC1/.

Acknowledgments

We thank J. Alonso, C. Bellini, M. Bennett, I. Blilou, J. Ecker, M. Estelle, J. Friml, H. Fukuda, N. Geldner, T. Guilfoyle, L. Hobbie, G. Jürgens, K. Koizumi, A. Molendijk, and R. Swarup for sharing materials. We acknowledge the Nottingham *Arabidopsis* Stock Centre for distributing SALK T-DNA insertion lines and other seed stocks. We acknowledge expert technical assistance from R. Granbom with root sectioning. We thank G. Samuelsson, O. Nilsson, A. Marchant, and A. Molendijk for discussion and comments and G. Sandberg for creating excellent scientific settings at UPSC. This work was supported by grants from the Swedish Research Council (Vetenskapsrådet) and the Swedish Foundation for Strategic Research (SSF).

Received: March 3, 2006
Revised: August 7, 2006
Accepted: August 30, 2006
Published: November 6, 2006

References

1. Strutt, H., and Strutt, D. (2005). Long-range coordination of planar polarity in *Drosophila*. Bioessays *27*, 1218–1227.
2. Grebe, M. (2004). Ups and downs of tissue and planar polarity in plants. Bioessays *26*, 719–729.
3. Masucci, J.D., and Schiefelbein, J.W. (1994). The *rhd6* mutation of *Arabidopsis thaliana* alters root hair initiation through an auxin- and ethylene-associated process. Plant Physiol. *106*, 1335–1346.
4. Grebe, M., Friml, J., Swarup, R., Ljung, K., Sandberg, G., Terlou, M., Palme, K., Bennett, M.J., and Scheres, B. (2002). Cell polarity signaling in *Arabidopsis* involves a BFA-sensitive auxin influx pathway. Curr. Biol. *12*, 329–334.
5. Sabatini, S., Beis, D., Wolkenfelt, H., Murfett, J., Guilfoyle, T., Malamy, J., Benfey, P., Leyser, O., Bechthold, N., Weisbeek, P., et al. (1999). An auxin-dependent distal organiser of pattern and polarity in the *Arabidopsis* root. Cell *99*, 463–472.
6. Marchant, A., Kargul, J., May, S.T., Muller, P., Delbarre, A., Perrot-Rechenmann, C., and Bennett, M.J. (1999). *AUX1* regulates root gravitropism in *Arabidopsis* by facilitating auxin uptake within root apical tissues. EMBO J. *18*, 2066–2073.
7. Yang, Y., Hammes, U.Z., Taylor, C.G., Schachtman, D.P., and Nielsen, E. (2006). High-affinity auxin transport by the AUX1 influx carrier protein. Curr. Biol. *16*, 1123–1127.
8. Alonso, J.M., Hirayama, T., Roman, G., Nourizadeh, S., and Ecker, J.R. (1999). EIN2, a bifunctional transducer of ethylene and stress responses in *Arabidopsis*. Science *284*, 2148–2152.
9. Steinmann, T., Geldner, N., Grebe, M., Mangold, S., Jackson, C.L., Paris, S., Gälweiler, L., Palme, K., and Jürgens, G. (1999). Coordinated polar localization of auxin efflux carrier PIN1 by GNOM ARF GEF. Science *286*, 316–318.
10. Molendijk, A.J., Bischoff, F., Rajendrakumar, C.S., Friml, J., Braun, M., Gilroy, S., and Palme, K. (2001). *Arabidopsis thaliana* Rop GTPases are localized to tips of root hairs and control polar growth. EMBO J. *20*, 2779–2788.
11. Jones, M.A., Shen, J.J., Fu, Y., Li, H., Yang, Z., and Grierson, C.S. (2002). The *Arabidopsis* Rop2 GTPase is a positive regulator of both root hair initiation and tip growth. Plant Cell *14*, 763–776.
12. Friml, J., Yang, X., Michniewicz, M., Weijers, D., Quint, A., Tietz, O., Benjamins, R., Ouwerker, P.B., Ljung, K., Sandberg, G., et al. (2004). A PINOID-dependent binary switch in apical-basal PIN polar targeting directs auxin efflux. Science *306*, 862–865.
13. Geldner, N., Anders, N., Wolters, H., Keicher, J., Kornberger, W., Muller, P., Delbarre, A., Ueda, T., Nakano, A., and Jürgens, G. (2003). The *Arabidopsis* GNOM ARF-GEF mediates endosomal recycling, auxin transport, and auxin-dependent plant growth. Cell *112*, 219–230.
14. Busch, M., Mayer, U., and Jürgens, G. (1996). Molecular analysis of the *Arabidopsis* pattern formation gene *GNOM*: gene structure and intragenic complementation. Mol. Gen. Genet. *250*, 681–691.
15. Koizumi, K., Sugiyama, M., and Fukuda, H. (2000). A series of novel mutants of *Arabidopsis thaliana* that are defective in the formation of continuous vascular network: calling the auxin signal flow canalization hypothesis into question. Development *127*, 3197–3204.
16. Delbarre, A., Muller, P., Imhoff, V., and Guern, J. (1996). Comparison of mechanisms controlling uptake and accumulation of 2,4-dichlorophenoxy acetic acid, naphthalene-1-acetic acid, and indole-3-acetic acid in suspension-cultured tobacco cells. Planta *198*, 532–541.
17. Hobbie, L., McGovern, M., Hurwitz, L.R., Pierro, A., Liu, N.Y., Bandyopadhyay, A., and Estelle, M. (2000). The *axr6* mutants of *Arabidopsis thaliana* define a gene involved in auxin response and early development. Development *127*, 23–32.
18. Friml, J., Vieten, A., Sauer, M., Weijers, D., Schwarz, H., Hamann, T., Offringa, R., and Jürgens, G. (2003). Efflux-dependent auxin gradients establish the apical-basal axis of Arabidopsis. Nature *426*, 147–153.
19. Delarue, M., Prinsen, E., van Onckelen, H., Caboche, M., and Bellini, C. (1998). *sur2* mutations of *Arabidopsis thaliana* define a new locus involved in the control of auxin homeostasis. Plant J. *14*, 603–611.
20. Kieber, J.J., Rothenberg, M., Roman, G., Feldmann, K.A., and Ecker, J.R. (1993). *CTR1*, a negative regulator of the ethylene response pathway in *Arabidopsis,* encodes a member of the raf family of protein kinases. Cell *72*, 427–441.
21. Stepanova, A.N., Hoyt, J.M., Hamilton, A.A., and Alonso, J.M. (2005). A link between ethylene and auxin uncovered by the characterization of two root-specific ethylene-insensitive mutants in *Arabidopsis*. Plant Cell *17*, 2230–2242.
22. Blilou, I., Xu, J., Wildwater, M., Willemsen, V., Paponov, I., Friml, J., Heidstra, R., Aida, M., Palme, K., and Scheres, B. (2005). The PIN auxin efflux facilitator network controls growth and patterning in *Arabidopsis* roots. Nature *433*, 39–44.
23. Knox, K., Grierson, C.S., and Leyser, H.M.O. (2003). AXR3 and SHY2 interact to regulate root hair development. Development *130*, 5769–5777.
24. Heidstra, R., Welch, D., and Scheres, B. (2004). Mosaic analyses using marked activation and deletion clones dissect *Arabidopsis SCARECROW* action in asymmetric cell division. Genes Dev. *18*, 1964–1969.
25. Eaton, S., Wepf, R., and Simons, K. (1996). Roles for Rac1 and Cdc42 in planar polarization and hair outgrowth in the wing of *Drosophila*. J. Cell Biol. *135*, 1277–1289.
26. Swarup, R., Kramer, E.M., Perry, P., Knox, K., Leyser, H.M.O., Haseloff, J., Beemster, G.T., Bhalerao, R., and Bennett, M.J. (2005). Root gravitropism requires lateral root cap and epidermal cells for transport and response to a mobile auxin signal. Nat. Cell Biol. *7*, 1057–1065.
27. Paciorek, T., Zazimalova, E., Ruthardt, N., Petrasek, J., Stierhof, Y.D., Kleine-Vehn, J., Morris, D.A., Emans, N., Jürgens, G., Geldner, N., et al. (2004). Auxin inhibits endocytosis and promotes its own efflux from cells. Nature *435*, 1251–1256.